

# Arteriosclerosis, Thrombosis, and Vascular Biology



JOURNAL OF THE AMERICAN HEART ASSOCIATION

## Aortic Reservoir Pressure Corresponds to Cyclic Changes in Aortic Volume: Physiological Validation in Humans

Martin G. Schultz, Justin E. Davies, Ashutosh Hardikar, Simon Pitt, Michela Moraldo, Niti Dhutia, Alun D. Hughes and James E. Sharman

*Arterioscler Thromb Vasc Biol.* 2014;34:1597-1603; originally published online May 8, 2014;  
doi: 10.1161/ATVBAHA.114.303573

*Arteriosclerosis, Thrombosis, and Vascular Biology* is published by the American Heart Association, 7272  
Greenville Avenue, Dallas, TX 75231

Copyright © 2014 American Heart Association, Inc. All rights reserved.  
Print ISSN: 1079-5642. Online ISSN: 1524-4636

The online version of this article, along with updated information and services, is located on the  
World Wide Web at:

<http://atvb.ahajournals.org/content/34/7/1597>

Data Supplement (unedited) at:

<http://atvb.ahajournals.org/content/suppl/2014/06/09/ATVBAHA.114.303573.DC1.html>

**Permissions:** Requests for permissions to reproduce figures, tables, or portions of articles originally published in *Arteriosclerosis, Thrombosis, and Vascular Biology* can be obtained via RightsLink, a service of the Copyright Clearance Center, not the Editorial Office. Once the online version of the published article for which permission is being requested is located, click Request Permissions in the middle column of the Web page under Services. Further information about this process is available in the [Permissions and Rights Question and Answer](#) document.

**Reprints:** Information about reprints can be found online at:  
<http://www.lww.com/reprints>

**Subscriptions:** Information about subscribing to *Arteriosclerosis, Thrombosis, and Vascular Biology* is online at:  
<http://atvb.ahajournals.org/subscriptions/>

# Aortic Reservoir Pressure Corresponds to Cyclic Changes in Aortic Volume

## Physiological Validation in Humans

Martin G. Schultz, Justin E. Davies, Ashutosh Hardikar, Simon Pitt, Michela Moraldo, Niti Dhutia, Alun D. Hughes, James E. Sharman

**Objective**—Aortic reservoir pressure indices independently predict cardiovascular events and mortality. Despite this, there has never been a study in humans to determine whether the theoretical principles of the mathematically derived aortic reservoir pressure ( $RP_{\text{derived}}$ ) and excess pressure ( $XP_{\text{derived}}$ ) model have a real physiological basis. This study aimed to directly measure the aortic reservoir ( $AR_{\text{direct}}$ ; by cyclic change in aortic volume) and determine its relationship with  $RP_{\text{derived}}$ ,  $XP_{\text{derived}}$  and aortic blood pressure (BP).

**Approach and Results**—Ascending aortic BP and Doppler flow velocity were recorded via intra-arterial wire in 10 men (aged  $62 \pm 12$  years) during coronary artery bypass surgery. Simultaneous ascending aortic transesophageal echocardiography was used to measure  $AR_{\text{direct}}$ . Published mathematical formulae were used to determine  $RP_{\text{derived}}$  and  $XP_{\text{derived}}$ .  $AR_{\text{direct}}$  was strongly and linearly related to  $RP_{\text{derived}}$  during systole ( $r=0.988$ ;  $P<0.001$ ) and diastole ( $r=0.985$ ;  $P<0.001$ ). Peak cross-correlation ( $r=0.98$ ) occurred at a phase lag of 0.004 s into the cardiac cycle, suggesting close temporal agreement between waveforms. The relationship between aortic BP and  $AR_{\text{direct}}$  was qualitatively similar to the cyclic relationship between aortic BP and  $RP_{\text{derived}}$  with peak cross-correlations occurring at identical phase lags ( $AR_{\text{direct}}$  versus aortic BP,  $r=0.96$  at 0.06 s;  $RP_{\text{derived}}$  versus aortic BP,  $r=0.98$  at 0.06 s).

**Conclusions**— $RP_{\text{derived}}$  is highly correlated with changes in proximal aortic volume, consistent with its physiological interpretation as corresponding to the instantaneous volume of blood stored in the aorta. Thus, aortic reservoir pressure should be considered in the interpretation of the central BP waveform. (*Arterioscler Thromb Vasc Biol.* 2014;34:1597-1603.)

**Key Words:** aorta ■ vascular stiffness

Central (aortic) blood pressure (BP) waveform indices independently predict cardiovascular events and all-cause mortality,<sup>1</sup> but the physiological mechanisms to explain the waveform morphology remain disputed. The well-established wave reflection theory ascribes transmission of discrete forward and backward (incident and reflected) waves as the principal contributory factor underlying the shape of the central BP waveform.<sup>2</sup> However, while providing a plausible description of central BP morphology, recent studies have concluded that the influence of discrete reflected waves on central BP may be less than originally conceived, and this is probably because of wave dispersion along the aorta and entrapment of reflected waves in the periphery.<sup>3,4</sup> Indeed, augmentation of central BP may be largely attributable to forward wave propagation (as a result of left ventricular [LV] ejection) and proximal aortic reservoir function.<sup>5-9</sup> Importantly, wave separation theory obscures the pressure

buffering role of the highly elastic proximal aorta (ie, the aortic reservoir), and a failure to consider this function may lead to incorrect interpretations of the physiology underlying central BP waveform morphology.

The reservoir-excess pressure concept is an alternate method proposed to explain the underlying physiology of the aortic BP waveform. This method has been used invasively to study changes in aortic BP associated with both aging and exercise.<sup>6,8</sup> Moreover, indices derived from this model were recently shown to predict cardiovascular events (fatal and nonfatal) and procedures independent from brachial BP and other conventional cardiovascular risk parameters (eg, age, sex, cholesterol, smoking, diabetes mellitus), including Framingham risk score, in an analysis of the Conduit Artery Function Evaluation study.<sup>10</sup> In accounting for the reservoir function of the aorta,<sup>7,11</sup> the reservoir-excess pressure model is founded on the basis that aortic BP can be separated into

Received on: January 13, 2014; final version accepted on: April 23, 2014.

From the Menzies Research Institute Tasmania, University of Tasmania, Hobart, Tasmania, Australia (M.G.S., A.H., J.E.S.); International Centre for Circulatory Health, Imperial College London, London, United Kingdom (J.E.D., M.M., N.D.); Royal Hobart Hospital, Hobart, Tasmania, Australia (S.P.); and Institute of Cardiovascular Science, University College London, London, United Kingdom (A.D.H.)

The online-only Data Supplement is available with this article at <http://atvb.ahajournals.org/lookup/suppl/doi:10.1161/ATVBAHA.114.303573/-DC1>.

Correspondence to James E. Sharman, PhD, Menzies Research Institute Tasmania, University of Tasmania, Private Bag 23, Hobart 7000, Tasmania, Australia. E-mail James.Sharman@menzies.utas.edu.au

© 2014 American Heart Association, Inc.

*Arterioscler Thromb Vasc Biol* is available at <http://atvb.ahajournals.org>

DOI: 10.1161/ATVBAHA.114.303573

### Nonstandard Abbreviations and Acronyms

$AR_{\text{direct}}$	aortic reservoir (measured)
BP	blood pressure
$RP_{\text{derived}}$	reservoir pressure (derived)
$XP_{\text{derived}}$	excess pressure (derived)

a volume-related reservoir pressure, which is theorized as representative of the cyclic volume increase (aortic distension) that occurs during systole (to store blood) and volume decrease (aortic recoil) during diastole (to discharge blood), as well as a wave-related (excess) pressure, which can be decomposed into incident and reflected waves.<sup>11</sup> The reservoir-excess pressure concept is underpinned by a mathematical construct,<sup>11–13</sup> in which derived aortic reservoir ( $RP_{\text{derived}}$ ) and excess pressure ( $XP_{\text{derived}}$ ) parameters are calculated from measured pressure with or without flow velocity. Although the reservoir pressure waveform derived from this model shows similarity to the estimated thoracic aortic volume curve in a dog model,<sup>11</sup> there has never been a study in humans to directly measure the aortic reservoir to determine whether the theoretical physiological principles are correct. Accordingly, this study aimed to measure the cyclic changes in aortic reservoir ( $AR_{\text{direct}}$ ) and compare this to  $RP_{\text{derived}}$ , as well as  $XP_{\text{derived}}$  and aortic BP. We hypothesized that there would be a close relationship between  $AR_{\text{direct}}$  and  $RP_{\text{derived}}$ , and that both would share a similar relationship with aortic BP.

### Materials and Methods

Materials and Methods are available in the online-only Supplement (Figures 1–3).<sup>14–16</sup>

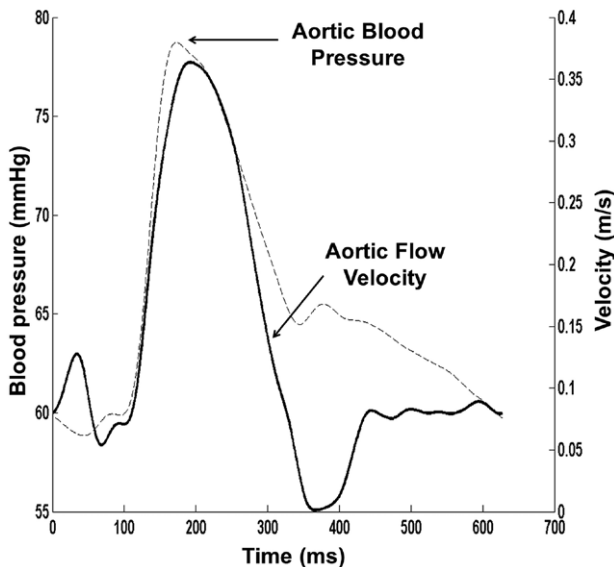


**Figure 1.** Example of ensemble averaged (6 beats) aortic blood pressure (broken line) and aortic flow velocity (solid line) recorded during coronary artery bypass graft surgery.

## Results

### Clinical Characteristics

The clinical details of study participants are presented in Table 1. All patients were undergoing coronary bypass grafting, and 1 patient was also having mitral valve repair. Most patients had hypertension or hyperlipidemia, and all were taking pharmacological agents, including antihypertensive, lipid lowering, antiplatelet, and aspirin medications. Three individuals had type 2 diabetes mellitus, for which 2 were receiving insulin therapy. There was a high prevalence of a family history of cardiovascular disease, smoking history, and 3 individuals had previous myocardial infarctions. Although 2 individuals had reduced LV ejection fraction (<50%), all patients were at the lower end of New York Heart Association functional classification. Data from 1 individual were excluded from analysis because of technical difficulty in appropriately tracking aortic wall changes, leaving 9 patients available for analysis of  $AR_{\text{direct}}$ .

### Hemodynamics

All hemodynamic variables are outlined in Table 2. Aortic pressures (systolic, diastolic, and mean arterial pressure) were maintained at low values during the surgery and research measurements and probably because of this augmentation pressure and augmentation index were also low.

### Relationship Between $AR_{\text{direct}}$ and $RP_{\text{derived}}$

$AR_{\text{direct}}$  was scaled to the same relative amplitude as  $RP_{\text{derived}}$ , and the relationship between the 2 variables was qualitatively similar (Figure 4A). When plotted together across 1 full cardiac cycle,  $AR_{\text{direct}}$  was significantly and linearly correlated to  $RP_{\text{derived}}$  from end diastole through to peak systole ( $r=0.988$ ;  $P<0.001$ ; Figure 4B, points 1–2) and from peak systole through to end diastole ( $r=0.985$ ;  $P<0.001$ ; Figure 4B, points 2–3). Overall, cross-correlation between  $AR_{\text{direct}}$  and  $RP_{\text{derived}}$  at zero phase shift was strong ( $r=0.97$ ). Peak cross-correlation (maximal concordance between waveforms) occurred at a phase lag of 0.004 s ( $r=0.98$ ; black dot, Figure 4C), indicating a strong temporal correspondence.

### Relationship Between $AR_{\text{direct}}$ and Aortic BP

$AR_{\text{direct}}$  was scaled to the same amplitude as aortic BP, and this relationship is shown in Figure 4D. When plotted together across a full cardiac cycle (Figure 4E), a rise in aortic BP from the onset of systole (Figure 4E, point 1) was observed, together with a corresponding (although less steep and somewhat lagged) increase in  $AR_{\text{direct}}$  that continued until peak systole (Figure 4E, point 2). From peak systole, aortic BP plateaued momentarily (while  $AR_{\text{direct}}$  continued to rise) before dropping until aortic valve closure at end systole. After closure of the aortic valve, both aortic BP and  $AR_{\text{direct}}$  decreased linearly to baseline levels at end diastole (Figure 4E, point 3). Cross-correlation between variables at zero phase shift was high ( $r=0.80$ ), with peak cross-correlation found at a phase lag of 0.06 s ( $r=0.96$ ; Figure 4F).

### Relationship Between $RP_{\text{derived}}$ and Aortic BP

To allow visual comparison,  $RP_{\text{derived}}$  was scaled to the same amplitude as aortic BP and is shown in Figure 4G. When plotted across 1 full cardiac cycle (Figure 4H), the relationship

between waveforms (Figure 4H, points 1–3) was qualitatively similar to that observed between aortic BP and  $AR_{direct}$  (as shown in Figure 4E). Cross-correlation at zero phase shift was identical to the overall magnitude of cross-correlation between aortic BP and  $AR_{direct}$  ( $r=0.80$ ). Peak cross-correlation between  $RP_{derived}$  and aortic BP occurred at a phase lag of 0.06 s ( $r=0.98$ ; Figure 4I), which was similar to the phase lag of peak cross-correlation of aortic BP and  $AR_{direct}$  (as shown in Figure 4F). These data suggest that  $RP_{derived}$  and  $AR_{direct}$  share similar temporal relationships with aortic BP.

## Discussion

In this study, we present the first physiological validation of the mathematically derived reservoir-excess pressure paradigm in man. Our primary finding demonstrates a significant linear relationship and strong temporal concordance between  $AR_{direct}$  and  $RP_{derived}$  waveforms. Adding to this,  $AR_{direct}$  and  $RP_{derived}$  shared the same relationship with aortic BP. Taken together, our results demonstrate that aortic reservoir pressure has a genuine, rather than just theoretical, physiological foundation as corresponding to the volume of blood stored in the aorta and emphasize the importance of the aortic reservoir in describing the morphology of the central BP waveform.

### Aortic Reservoir and Excess Pressure: A Physiological Paradigm

The reservoir-excess pressure concept has evolved from wave intensity analysis as a time domain technique to study arterial hemodynamics.<sup>7,11,13,17–19</sup> As a mathematical model, the decomposition of central BP into reservoir and excess pressure components (derived from measured pressure and flow velocity) has proved a useful<sup>7</sup> and valid technique<sup>12</sup> to describe the central BP waveform and also seems to overcome some conceptual limitations of traditional wave-only models to

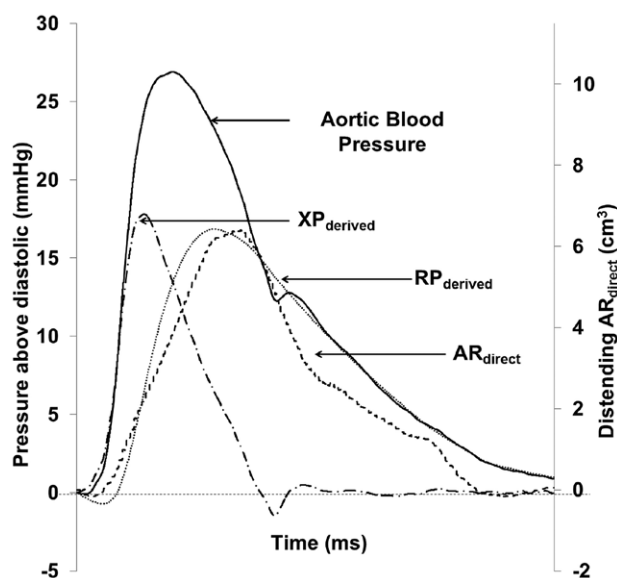


**Figure 2.** Overlay of average aortic blood pressure (solid line), aortic reservoir ( $AR_{direct}$ ; dashed line), reservoir pressure ( $RP_{derived}$ ; dotted line), and excess pressure ( $XP_{derived}$ ; dash-dot line) waveforms across 1 cardiac cycle. All waveforms have been aligned using the peak R wave on ECG as a fiducial point.

explain central BP waveform morphology.<sup>11,17,18,20</sup> For the first time, this study shows that the idea of the aortic reservoir as a volume-related pressure component also has physiological merit in man.

Reservoir pressure (and volume) must rise during systole because aortic inflow exceeds aortic outflow, resulting in distension of the vessel wall (storing potential energy) and an increase in aortic volume. Our results confirm this idea because both  $AR_{direct}$  (our direct volume measure) and  $RP_{derived}$  (theoretical reservoir pressure) rose almost in unison through systole (Figure 4A and 4B). As expected,  $AR_{direct}$  and  $RP_{derived}$  increased more gradually in comparison with aortic BP in this study. Although others have suggested that a strict linear

### A AORTIC SEGMENT LENGTH = distance A to B (cm)

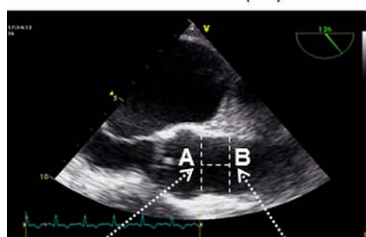
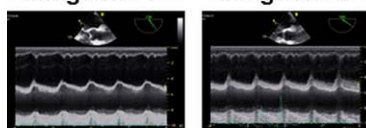
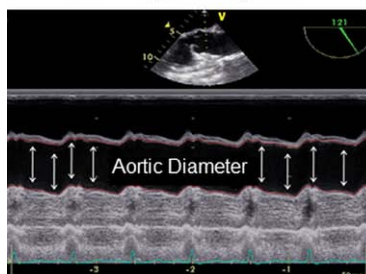


Image site 1

Image site 2



### B AORTIC DIAMETER custom edge tracking software



### C AORTIC VOLUME

$$= l\pi r^2$$

where  $l$  = segment length,  $r$  = diameter/2

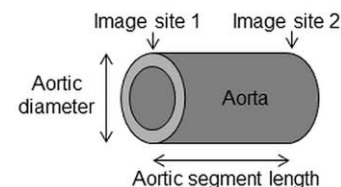


**Figure 3.** Illustration of the 3 step process involved in determining aortic reservoir ( $AR_{direct}$ ). **A**, Process of determining aortic segment length, showing a 2-dimensional image of the proximal aorta, with aortic segment length corresponding to the distance between the 2 sites of M-mode image measurements indicated as A and B (top), with the 2 M-mode recordings from locations A and B, respectively, shown at the bottom. **B**, An M-mode image and the customized edge tracking software were used to determine cyclic changes in aortic diameter. **C**, With aortic segment length and diameter known, aortic volume ( $AR_{direct}$ ) was calculated using the formula for the volume of a cylinder.

**Table 1. Clinical Characteristics of Study Participants**

Male sex	10 (100)
Age, y	62±12
Height, cm	175±4
Weight, kg	87±12
Body mass index, kg/m <sup>2</sup>	28±5
NYHA functional classification 1	3 (30)
NYHA functional classification 2	6 (60)
NYHA functional classification 3	1 (10)
LVEF <50%	2 (20)
Surgery performed	
CABG×1	1 (10)
CABG×2	2 (20)
CABG×3	4 (40)
CABG×4	2 (20)
CABG×5	1 (10)
Mitral valve repair	1 (10)
Previous myocardial infarction	3 (30)
Hypertension	9 (90)
Type 2 diabetes mellitus	3 (30)
Chronic kidney disease	1 (10)
Smoking history (no/former/current)	3 (30)/5 (50)/2 (20)
Family history of CVD	5 (50)
Hyperlipidemia	8 (80)
Pharmacological therapy	
Lipid lowering	8 (80)
Aspirin	8 (80)
Calcium channel blocker	1 (10)
β-Blocker	5 (50)
Angiotensin-converting enzyme inhibitor	4 (40)
Angiotensin receptor blocker	3 (30)
Antiplatelet	5 (50)
Diuretic	2 (20)
Digoxin	1 (10)
Insulin	2 (20)

Data are mean±SD or n (%). n=10. CABG indicates coronary artery bypass graft; CVD, cardiovascular disease; LVEF, left ventricular ejection fraction; and NYHA, New York Heart Association.

relationship exists between aortic BP and dimensions,<sup>21</sup> our findings lend credence to more recent literature that describes a hysteretic (loop) relationship between aortic BP and dimensions.<sup>22–24</sup> Physiologically, this makes sense because there must be a delay in the volumetric increase (relative to pressure), while the aorta fills with blood (Figure 4D–4I). Importantly, however, a large proportion of the pressure from the column of blood ejected into the arterial network during systole is dampened within the ascending aorta via the reservoir function (≤37%).<sup>25</sup> This buffer role in mitigating cyclic pulsatile fluctuations in BP ensures a more steady flow of blood at the peripheral tissue level and maintains outflow in diastole. After closure of the aortic valve, the aorta recoils (releasing the stored energy) as blood discharges from the

**Table 2. Measured and Calculated Hemodynamic Parameters of Study Participants**

Aortic systolic pressure, mm Hg	84±7
Aortic diastolic pressure, mm Hg	59±8
Mean arterial pressure, mm Hg	68±6
Aortic pulse pressure, mm Hg	25±9
Augmentation pressure, mm Hg	−1±2
Augmentation index, %	−3±7
Heart rate, bpm	75±16
Peak aortic flow velocity, cm/s	52±12
Aortic wave speed, m/s	5.3±1.5
Peak AR <sub>direct</sub> cm <sup>3</sup>	17±9
Peak RP <sub>derived</sub> mm Hg	75±8
Peak XP <sub>derived</sub> mm Hg	68±5
Integral RP <sub>derived</sub> Pa.s	6×10 <sup>5</sup> ±3×10 <sup>5</sup>
Integral XP <sub>derived</sub> Pa.s	5×10 <sup>5</sup> ±3×10 <sup>5</sup>

Data are mean±SD; n=9. AR indicates aortic reservoir; bpm, beats per minute; RP, reservoir pressure; and XP, excess pressure.

proximal aorta into the distal vasculature throughout diastole. At this time, aortic outflow exceeds the inflow (there is no source of continued inflow to the aorta after aortic valve closure), and aortic volume and reservoir pressure decline. Again, this aspect of reservoir function can be observed in our data, as AR<sub>direct</sub> and RP<sub>derived</sub> waveforms decline in proportion to each other and aortic BP during diastole (Figure 4). The gradual decline in reservoir pressure through diastole will maintain diastolic coronary perfusion pressure, while negating the requirement for self-canceling reflected waves that are implicit with wave reflection theory.<sup>7</sup>

Aortic reservoir pressure is theorized as the minimum work that the contracting LV must achieve to eject blood into the aorta,<sup>19</sup> and the magnitude of aortic reservoir pressure is highly dependent on the compliance of the vessel. Under optimal conditions, the elasticity of the proximal ascending aorta plays an important role in minimizing excessive pulsatility in BP and LV power expenditure.<sup>26</sup> However, when compliance is reduced (ie, when reservoir function is impaired), some of the pressure buffering capacity is diminished and aortic BP may become elevated because of a more rapid increase in reservoir pressure for a similar rise in aortic volume.<sup>17,25</sup> This hemodynamic consequence has been demonstrated in animal studies whereby application of non-compliant grafts around (or in replacement of) the proximal aorta acutely yields more pathological central BP waveforms (augmented BP) and increased myocardial load resulting in LV hypertrophy.<sup>27–29</sup> It is, therefore, not surprising that as the large arteries become stiff with age,<sup>30</sup> the altered aortic reservoir function largely accounts for the augmentation of the central BP waveform.<sup>6</sup>

Once the reservoir function of the aorta is considered, the remaining contribution to the central BP waveform (the excess pressure) has been proposed to correspond to the excess LV work beyond the minimum needed for flow ejection into the proximal aorta.<sup>19</sup> Our data lend support to this idea because the addition of XP<sub>derived</sub> to RP<sub>derived</sub> (forming total pressure)

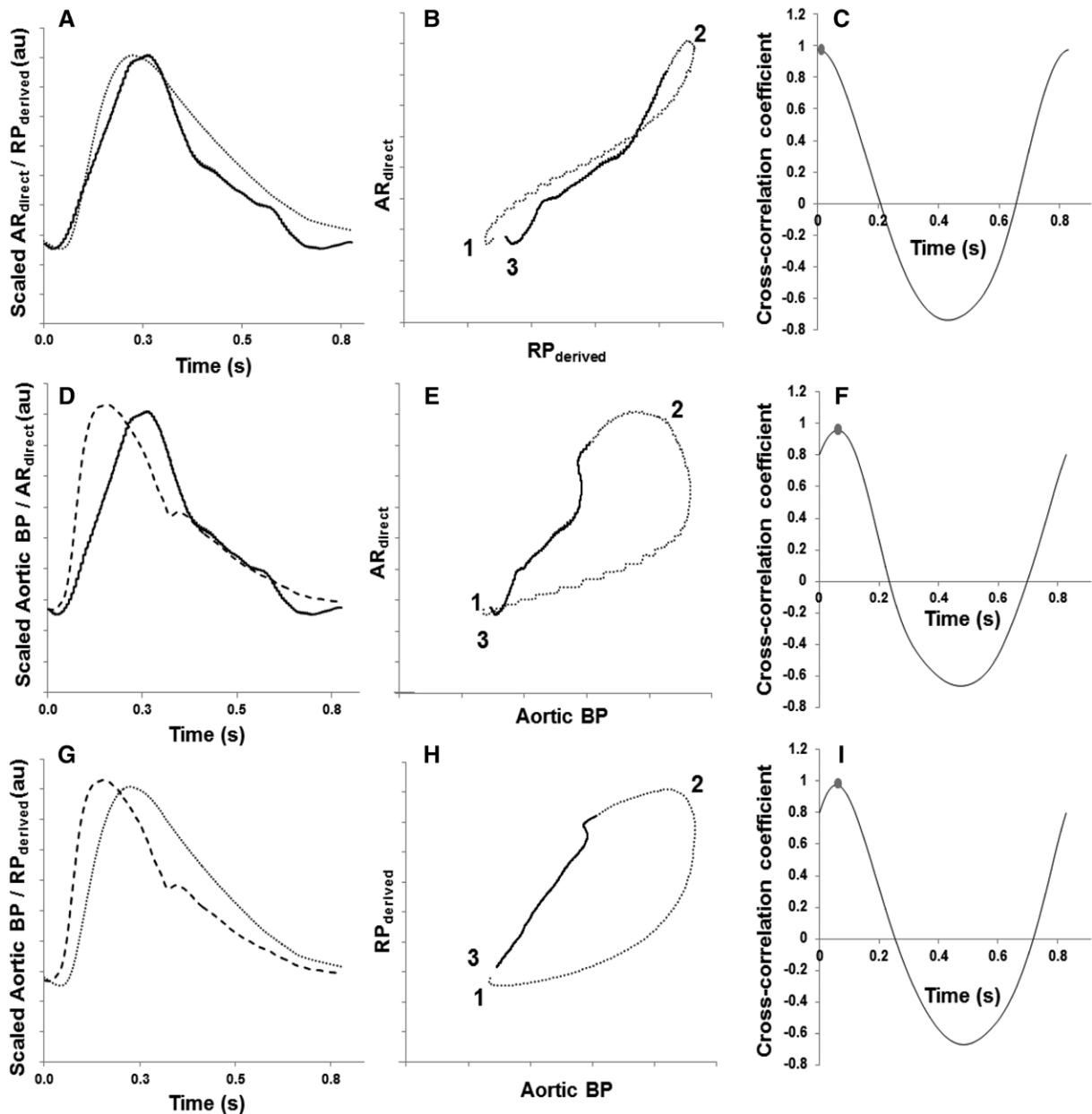


**Figure 4.** Averaged, combined ( $n=9$ ), and scaled waveforms depicting the relationship between (A) aortic reservoir ( $AR_{direct}$ ; solid line) and aortic reservoir pressure ( $RP_{derived}$ ; dotted line), (D) aortic blood pressure (BP; dashed line) and  $AR_{direct}$ , and (G) aortic BP and  $RP_{derived}$  (dotted line) across 1 full cardiac cycle. Each relationship (B, E, and H) is then plotted through both systole (broken lines) and diastole (solid lines). Numbers represent events through the cardiac cycle, including aortic valve opening (1), peak systole (2), and end diastole (3). Cross-correlation plots (C, F, and I) are also shown for each relationship, with the time (phase lag) of peak cross-correlation denoted by the black dot.

changed the linear relationship observed between  $AR_{direct}$  and  $RP_{derived}$  (Figure 4B) into the hysteretic relationship observed in Figure 4E. Thus, the energy associated with excess pressure that is lost to hysteresis may, at least in part, reflect myocardial or circulatory inefficiency, as described by Parker et al.<sup>19</sup> These inefficiencies could have clinical relevance beyond conventional cardiovascular risk factors. Indeed, such evidence was recently reported from the Conduit Artery Function Evaluation study, where excess pressure integral was shown to independently predict cardiovascular events.<sup>10</sup> The excess pressure waveform has also been consistently shown to bear striking resemblance to the flow velocity trace in the ascending aorta,<sup>6,7,11,17</sup> representative

of LV stroke volume.<sup>20</sup> With regard to Figure 2, it is  $XP_{derived}$  that first rapidly rises with aortic pressure, before  $AR_{direct}$  and  $RP_{derived}$  (ie, reservoir pressure) more gradually begin to increase as the aorta distends and volume increases. This is also consistent with the notion that the cardiovascular system is designed to favor forward blood flow, minimizing resistance caused by reflected wave energy in the proximal aorta during systole. Changes in excess pressure, or stroke volume, may, therefore, have a pivotal role in determining the shape of the central BP waveform. Indeed, beat-to-beat variation in augmentation pressure, most likely caused by respiratory variation in LV filling (and ejection) patterns, has been observed previously.<sup>31</sup>

### Central BP Waveform Morphology: Discrete Wave Reflection or Reservoir Function?

The morphology of the central BP waveform has long been described in the frequency domain as emanating from discrete outgoing and reflected waves.<sup>2,32,33</sup> With each cardiac ejection, a forward propagating wave is transmitted through the arteries toward the periphery. At sites of potential impedance mismatch, part of this wave energy is reflected back toward the heart, resulting in augmentation of central BP if arriving during systole. The time of arrival and magnitude of this reflected wave are posited as the sole contributor to the augmentation of the central BP waveform.<sup>2,34</sup> Although generally accepted, this traditional explanation of central BP morphology does not take into consideration the reservoir function of the proximal aorta, a function that this study has confirmed is physiological.

Beyond this study, mounting evidence suggests that discrete wave reflection has a less important role in determining the shape of the central BP waveform than originally conceived.<sup>3,4,6,8,35</sup> Although some reflected wave energy is clearly evident from wave intensity data captured in the human ascending aorta,<sup>4,8</sup> there seems to be no dramatic shift in reflected wave timing (moving from diastole into systole) that is said to occur with central BP augmentation associated with aging.<sup>35</sup> Indeed, age changes in central BP augmentation are perhaps more likely related to reductions in aortic compliance and reservoir function.<sup>6</sup> Other studies also describe a horizon effect on wave travel, whereby reflected waves become trapped in the periphery or dispersed along the length of the aorta.<sup>3,4</sup> Our recent work is also consistent with a less prominent role for wave reflection because despite significant augmentation of BP during exercise, reflected wave intensity effectively remains unchanged from resting conditions.<sup>8</sup>

### Limitations

This study was conducted in a small sample of participants, who were of older age, under treatment with a number of pharmacological agents, and with significant coronary artery lesions requiring surgery. Moreover, because of the surgical procedure, it was necessary to maintain low BP by pharmacological means resulting in relatively high-flow output with minimal resistance because of peripheral vasodilation. This limited our capacity to examine the influence of higher pressures on aortic reservoir characteristics, where there would be an expectation of a nonlinear decrease in aortic compliance (with transfer of load bearing from elastin to stiffening collagen fibers),<sup>36</sup> and increased augmented pressure. Therefore, the relevance of our findings to the hemodynamic milieu of high arterial pressure, or cardiovascular pathologies different from those studied in this work, is unknown. It is also possible that small errors in the measurement of aortic diameter may have magnified error in calculation of volume ( $AR_{\text{direct}}$ ). Additionally, the averaging of  $AR_{\text{direct}}$  may have induced bias owing to averaging filtering of some waveform features. However, the morphology of diameter and volumetric waveforms were consistent with those measured by others, suggesting this was not a major issue.

### Conclusions

This study demonstrates that the aortic reservoir has a meaningful physiological interpretation and adds to a growing body of literature revealing the importance of aortic reservoir function to explain the morphology of the central BP waveform. Further studies to determine the clinical relevance and prognostic use of aortic reservoir function and excess pressure are needed.

### Sources of Funding

This study was supported by a grant-in-aid from the National Heart Foundation of Australia (G11H5915). Dr Schultz received support from Exercise and Sports Science Australia Tom Penrose research grant, 2009. Dr Sharman was supported by a Career Development Award from the National Health and Medical Research Council of Australia (569519). Professor Hughes and Dr Davies received support from the UK National Institute for Health Research Biomedical Research Centre Scheme and the British Heart Foundation Centre of Research Excellence Award to Imperial College London.

### Disclosures

None.

### References

- Vlachopoulos C, Aznaouridis K, O'Rourke MF, Safar ME, Baou K, Stefanadis C. Prediction of cardiovascular events and all-cause mortality with central haemodynamics: a systematic review and meta-analysis. *Eur Heart J*. 2010;31:1865–1871.
- Nichols WW, O'Rourke MF. *McDonald's Blood Flow in Arteries: Theoretical, Experimental and Clinical Principles*. London, UK: Hodder Arnold; 2005.
- Hope SA, Tay DB, Meredith IT, Cameron JD. Waveform dispersion, not reflection, may be the major determinant of aortic pressure wave morphology. *Am J Physiol Heart Circ Physiol*. 2005;289:H2497–H2502.
- Davies JE, Alastruey J, Francis DP, Hadjiloizou N, Whinnett ZI, Manisty CH, Aguado-Sierra J, Willson K, Foale RA, Malik IS, Hughes AD, Parker KH, Mayet J. Attenuation of wave reflection by wave entrapment creates a "horizon effect" in the human aorta. *Hypertension*. 2012;60:778–785.
- Cheng K, Cameron JD, Tung M, Mottram PM, Meredith IT, Hope SA. Association of left ventricular motion and central augmentation index in healthy young men. *J Hypertens*. 2012;30:2395–2402.
- Davies JE, Baksi J, Francis DP, Hadjiloizou N, Whinnett ZI, Manisty CH, Aguado-Sierra J, Foale RA, Malik IS, Tyberg JV, Parker KH, Mayet J, Hughes AD. The arterial reservoir pressure increases with aging and is the major determinant of the aortic augmentation index. *Am J Physiol Heart Circ Physiol*. 2010;298:H580–H586.
- Davies JE, Hadjiloizou N, Leibovich D, Malaweera A, Alastruey-Armon J, Whinnett ZI, Manisty CH, Francis DP, Aguado-Sierra J, Foale RA, Malik IS, Parker KH, Mayet J, Hughes AD. Importance of the aortic reservoir in determining the shape of the arterial pressure waveform – the forgotten lessons of Frank. *Artery Research*. 2007;1:40–45.
- Schultz MG, Davies JE, Roberts-Thomson P, Black JA, Hughes AD, Sharman JE. Exercise central (aortic) blood pressure is predominantly driven by forward traveling waves, not wave reflection. *Hypertension*. 2013;62:175–182.
- Sharman JE, Davies JE, Jenkins C, Marwick TH. Augmentation index, left ventricular contractility, and wave reflection. *Hypertension*. 2009;54:1099–1105.
- Davies JE, Lacy P, Tillin T, Collier D, Cruikshank JK, Francis DP, Malaweera A, Mayet J, Stanton A, Williams B, Parker KH, Thom SA, Hughes AD. Excess pressure integral predicts cardiovascular events independent of other risk factors in the Conduit Artery Functional Evaluation (CAFE) sub-study of Anglo-Scandinavian Cardiac Outcomes Trial (ASCOT). *Hypertension*. In press.
- Wang JJ, O'Brien AB, Shrive NG, Parker KH, Tyberg JV. Time-domain representation of ventricular-arterial coupling as a windkessel and wave system. *Am J Physiol Heart Circ Physiol*. 2003;284:H1358–H1368.
- Sridharan SS, Burrowes LM, Bouwmeester JC, Wang JJ, Shrive NG, Tyberg JV. Classical electrical and hydraulic Windkessel models validate

- physiological calculations of Windkessel (reservoir) pressure. *Can J Physiol Pharmacol.* 2012;90:579–585.
13. Wang JJ, Shrive NG, Parker KH, Hughes AD, Tyberg JV. Wave propagation and reflection in the canine aorta: analysis using a reservoir-wave approach. *Can J Cardiol.* 2011;27:389.e1–389.10.
  14. Davies JE, Whinnett ZI, Francis DP, Willson K, Foale RA, Malik IS, Hughes AD, Parker KH, Mayet J. Use of simultaneous pressure and velocity measurements to estimate arterial wave speed at a single site in humans. *Am J Physiol Heart Circ Physiol.* 2006;290:H878–H885.
  15. Abel FL. Maximal negative dP/dt as an indicator of end of systole. *Am J Physiol.* 1981;240:H676–H679.
  16. Nelson-Wong E, Howarth S, Winter DA, Callaghan JP. Application of autocorrelation and cross-correlation analyses in human movement and rehabilitation research. *J Orthop Sports Phys Ther.* 2009;39:287–295.
  17. Tyberg JV, Davies JE, Wang Z, Whitelaw WA, Flewitt JA, Shrive NG, Francis DP, Hughes AD, Parker KH, Wang JJ. Wave intensity analysis and the development of the reservoir-wave approach. *Med Biol Eng Comput.* 2009;47:221–232.
  18. Wang JJ, Bouwmeester JC, Belenkie I, Shrive NG, Tyberg JV. Alterations in aortic wave reflection with vasodilation and vasoconstriction in anaesthetized dogs. *Can J Cardiol.* 2013;29:243–253.
  19. Parker KH, Alastruey J, Stan GB. Arterial reservoir-excess pressure and ventricular work. *Med Biol Eng Comput.* 2012;50:419–424.
  20. Tyberg JV, Bouwmeester JC, Shrive NG, Wang JJ. CrossTalk opposing view: forward and backward pressure waves in the arterial system do not represent reality. *J Physiol.* 2013;591(Pt 5):1171–3; discussion 1175.
  21. Patel DJ, De Freitas FM, Greenfield JC Jr, Fry DL. Relationship of radius to pressure along the aorta in living dogs. *J Appl Physiol.* 1963;18:1111–1117.
  22. Ferguson JJ 3rd, Momomura S, Sahagian P, Miller MJ, McKay RG. The use of nitroprusside to characterize aortic pressure-diameter relationships. *Tex Heart Inst J.* 1989;16:5–10.
  23. Ferguson JJ 3rd, Miller MJ, Sahagian P, Aroesty JM, McKay RG. Assessment of aortic pressure-volume relationships with an impedance catheter. *Cathet Cardiovasc Diagn.* 1988;15:27–36.
  24. Stefanadis C, Stratos C, Vlachopoulos C, Marakas S, Boudoulas H, Kallikazaros I, Tsiamis E, Toutouzas K, Sioros L, Toutouzas P. Pressure-diameter relation of the human aorta. A new method of determination by the application of a special ultrasonic dimension catheter. *Circulation.* 1995;92:2210–2219.
  25. Wang JJ, Shrive NG, Parker KH, Tyberg JV. Effects of vasoconstriction and vasodilatation on LV and segmental circulatory energetics. *Am J Physiol Heart Circ Physiol.* 2008;294:H1216–H1225.
  26. Kass DA. Ventricular arterial stiffening: integrating the pathophysiology. *Hypertension.* 2005;46:185–193.
  27. Kelly RP, Tunin R, Kass DA. Effect of reduced aortic compliance on cardiac efficiency and contractile function of in situ canine left ventricle. *Circ Res.* 1992;71:490–502.
  28. Ioannou CV, Stergiopoulos N, Katsamouris AN, Startchik I, Kalangos A, Licker MJ, Westerhof N, Morel DR. Hemodynamics induced after acute reduction of proximal thoracic aorta compliance. *Eur J Vasc Endovasc Surg.* 2003;26:195–204.
  29. Ioannou CV, Morel DR, Katsamouris AN, Katranitsa S, Startchik I, Kalangos A, Westerhof N, Stergiopoulos N. Left ventricular hypertrophy induced by reduced aortic compliance. *J Vasc Res.* 2009;46:417–425.
  30. AlGhatrif M, Strait JB, Morrell CH, Canepa M, Wright J, Elango P, Scuteri A, Najjar SS, Ferrucci L, Lakatta EG. Longitudinal trajectories of arterial stiffness and the role of blood pressure: the Baltimore Longitudinal Study of Aging. *Hypertension.* 2013;62:934–941.
  31. Schultz M, Davies J, Hughes A, Sharman J. Acute respiratory changes in augmentation index are related to aortic reservoir function. *Artery Research.* 2012;6:175
  32. Womersley JR. Method for the calculation of velocity, rate of flow and viscous drag in arteries when the pressure gradient is known. *J Physiol.* 1955;127:553–563.
  33. Segers P, Rietzschel ER, De Buyzere ML, Vermeersch SJ, De Bacquer D, Van Bortel LM, De Backer G, Gillebert TC, Verdonck PR; Asklepios investigators. Noninvasive (input) impedance, pulse wave velocity, and wave reflection in healthy middle-aged men and women. *Hypertension.* 2007;49:1248–1255.
  34. O'Rourke MF, Nichols WW. Aortic diameter, aortic stiffness, and wave reflection increase with age and isolated systolic hypertension. *Hypertension.* 2005;45:652–658.
  35. Baksi AJ, Treibel TA, Davies JE, Hadjiloizou N, Foale RA, Parker KH, Francis DP, Mayet J, Hughes AD. A meta-analysis of the mechanism of blood pressure change with aging. *J Am Coll Cardiol.* 2009;54:2087–2092.
  36. Armentano RL, Levenson J, Barra JG, Fischer EI, Breitbart GJ, Pichel RH, Simon A. Assessment of elastin and collagen contribution to aortic elasticity in conscious dogs. *Am J Physiol.* 1991;260(6 Pt 2):H1870–H1877.

### Significance

Aortic reservoir pressure indices independently predict cardiovascular events and mortality, but, until this study, it was unknown whether the theoretical principles of the aortic reservoir-excess pressure model have a real physiological basis in humans. Findings provide a physiological validation of the reservoir-excess pressure model in humans and represent an important advance in understanding central blood pressure physiology. Results also confirm that aortic reservoir pressure should be considered as a contributory factor toward the morphology of the central pressure waveform.

## **SUPPLEMENTARY MATERIAL**

### **Aortic reservoir pressure corresponds to cyclic changes in aortic volume: physiological validation in humans**

Martin G. SCHULTZ,<sup>1</sup> Justin E. DAVIES,<sup>2</sup> Ashutosh HARDIKAR,<sup>1</sup> Simon PITT,<sup>3</sup>  
Michela MORALDO,<sup>2</sup> Niti DHUTIA,<sup>2</sup> Alun D. HUGHES,<sup>4</sup> and James E. SHARMAN.<sup>1</sup>

(1) Menzies Research Institute Tasmania, University of Tasmania, Hobart, AUSTRALIA

(2) International Centre for Circulatory Health, Imperial College London, London, UK

(3) Royal Hobart Hospital, Hobart, AUSTRALIA

(4) Institute of Cardiovascular Science, University College London, London UK

## Materials and Methods

**Study participants.** Twelve male patients scheduled to undergo coronary artery bypass graft surgery at the Royal Hobart Hospital, Hobart, Australia were recruited for participation. Patients with aortic valve disease were excluded, due to the potential disturbance of normal proximal aortic haemodynamics. Power calculations were estimated on the basis of an expectation for a strong association between  $AR_{\text{direct}}$  and  $RP_{\text{derived}}$ , and we determined *a priori* that only 10 individuals were required to detect a conservative but significant ( $P < 0.05$ ) linear relationship between these variables ( $r \geq 0.75$ , with  $\alpha = 0.05$ ,  $1 - \beta = 0.80$ ). From the 12 patients consented to participate, data from two individuals was excluded due to technical difficulties encountered during data acquisition.

**Study protocol.** Patients were prepared for coronary artery bypass graft surgery in accordance with standard clinical care. General anaesthesia was induced with fentanyl and midazolam, aiming for a mean arterial pressure (MAP) of 60-70 mmHg. Each patient was subsequently intubated and ventilated with a tidal volume of 7-8 ml/kg of body weight. A mid sternotomy was performed and the pericardium was opened to expose the ascending aorta. Prior to administration of cardioplegia and cannulation of the proximal aortic arch, the cardioplegia suture site was chosen at the point of maximum convexity of the ascending aorta, which coincided with its mid portion (in front of the right pulmonary artery). This cardioplegia purse string was used to pass a percutaneous entry needle into the ascending aorta. Via this entry site, haemodynamic measurement of ascending aortic BP and flow velocity was made by intra-arterial wire, and utilised to calculate  $RP_{\text{derived}}$ . Simultaneous transesophageal echocardiography of the cyclic changes in proximal aortic volume was performed to determine  $AR_{\text{direct}}$  at the same site of  $RP_{\text{derived}}$  measurement. Patient clinical characteristics were extracted from medical records. The study received ethical approval from the Tasmanian Human Research Ethics Committee, and all patients provided written informed consent prior to participation.

**Hemodynamic data.** Aortic BP and flow velocity were recorded in the ascending aorta by intra-arterial pressure and Doppler flow velocity wire (single-use, 0.014", straight tip, Combwire, Volcano Therapeutic Corp, Rancho Cordova, CA, USA). Direct access to the ascending aorta was made via a 21g/4cm entry needle (Cook Medical, Bloomington, IL, USA). The Combwire was advanced beyond the needle tip for a distance of 2 cm so that the tip remained in the ascending aorta. The catheter position was also confirmed on transesophageal echocardiography, and small movements of the Combwire were made in order to obtain optimal flow velocity and pressure traces (see Figure 1 for example). Digital conversion of the pressure and flow velocity analogue outputs was made using PowerLab ML870 8/30, (AD Instruments, Bella Vista, Australia) and recorded using LabChart 7 software (AD Instruments, Bella Vista, Australia). Data was acquired at the sampling rate of 1000 Hz and simultaneous three lead electrocardiograph recording was made to calculate heart rate. Calibration of haemodynamic signals was performed offline using a two-point calibration method as previously described.<sup>1</sup>

Aortic BP and flow velocity traces corresponding exactly to the capture period of each aortic image were ensemble averaged offline for up to 6 heart cycles. Aortic systolic BP was defined as the maximum pressure point and diastolic BP was the minimum pressure point on the waveform. Aortic pulse pressure (PP) was defined as the difference between systolic and diastolic BP. Augmentation pressure (AP, systolic BP – pressure at the first inflection point) was calculated using a Matlab written program. Augmentation index (AIx) was calculated

from AP as a percentage of the overall PP. The sum of squares method was used to determine aortic wave speed, as previously described.<sup>2</sup>

**Transesophageal echocardiography.** Images of the ascending aorta were captured using a General Electric ultrasound machine (Vivid i, GE Medical Systems, Milwaukee, WI, USA) with a 6T-RS (2.9 – 6.7 MHz) transesophageal echocardiography probe. The probe was inserted under general anaesthesia into the upper oesophagus for imaging of the proximal aorta (image site 1), before being retracted to image a more distal location along the ascending aorta (image site 2). For each imaging site, over several cardiac cycles (typically up to six beats), a long axis two dimensional motion clip and m-mode image was acquired by imaging around the 120° plane, followed by the same images in short axis by imaging around the 30° plane. Appropriate gain, high frequency settings, narrow sector widths and minimum sector depths were used to optimise the image quality. Movement artefact was minimised by brief (<10 seconds) periods of apnoea when patients oxygenation and ventilation safely permitted. Short and long axis two dimensional and m-mode images were saved in mpeg and bmp formats respectively for offline analysis. All imaging was performed simultaneously with hemodynamic measurements.

**RP<sub>derived</sub> and XP<sub>derived</sub>.** RP<sub>derived</sub> was calculated using both pressure and flow by the previously published Equation 1,<sup>3, 4</sup> where  $P_{\infty}$  is the pressure asymptote at which flow through the microcirculation is assumed to be negligible,  $Q_{in}$  is the flow into the aorta,  $P_d$  is the diastolic pressure at maximum negative derivative of pressure (max  $-dp/dt$ ) after the peak pressure which is assumed to correspond to the beginning of diastole,<sup>5</sup>  $R$  is the resistance to aortic outflow as a result of downstream impedance,  $C$  is the compliance of the reservoir and  $\tau$  is the time constant of the exponential decline in pressure in diastole. XP<sub>derived</sub> was calculated by subtracting RP<sub>derived</sub> from aortic BP, and represents the wave component of pressure composed of both forward and backward propagating waves. Using customised algorithms, separation of aortic BP into both RP<sub>derived</sub> and XP<sub>derived</sub> was performed in Matlab (Mathworks, Natick, MA) on ensemble averaged aortic BP (over the aortic imaging periods), and by using a continuous, beat-to-beat separation analysis (again over the aortic imaging periods) to allow beat matched comparison with the AR<sub>direct</sub> and aortic BP (see Figure 2 for example).

### Equation 1

$$P_{\text{reservoir}} - P_{\infty} = \frac{e^{-t/RC}}{C} \int_0^t Q_{in}(t') e^{t'/RC} dt' + (P_d - P_{\infty}) e^{-t/RC}$$

**AR<sub>direct</sub>.** A direct measure of aortic reservoir was made offline in a three step process. Firstly, measurement of the distance between the two echocardiography imaging sites (aortic segment length) was made. All segment length measures were performed on a two dimensional image, where both image capture sites were clearly visible. Accuracy of segment length measures was achieved by visualising landmarks relative to the capture sites on both long axis m-mode images, which were open at the time of all length measures. Repeat length measurements were made between the two imaging sites on the anterior wall, posterior wall and the central lumen. The average of the two central lumen measurements was treated as the aortic segment length (see Figure 3 for example). The average aortic segment length was 1.5

$\pm 0.7$  cm. Secondly; the cyclic changes in aortic diameter were calculated using a custom written, automated wall-tracking algorithm with visual inspection to confirm appropriate tracking. The best quality m-mode echocardiography image (short or long axis) captured from either the proximal or distal end of the aortic segment was chosen to make all measurements. Once a quality wall tracking was achieved, data points for both the posterior and anterior aortic wall were exported for analysis. To calculate the cyclic changes in diameter, the anterior wall trace was inverted offline so that a delta lumen (diameter) waveform could be plotted. The diameter was not significantly different between the proximal and distal ends (imaging sites) of the aortic segment, and thus we considered the segment to be a right circular cylinder. Finally, with both aortic diameter and segment length known,  $AR_{\text{direct}}$  was calculated using the formula to determine the volume of a cylinder ( $l\pi r^2$ ; where  $l$  was the aortic segment length between imaging sites 1 and 2; and  $r$ , was the delta aortic lumen diameter / 2). A representative  $AR_{\text{direct}}$  waveform of one cardiac cycle from each individual was first ensemble averaged, and then combined with all study participants to derive an average  $AR_{\text{direct}}$  waveform used in all analysis. This averaging process was also completed for measured aortic pressure,  $RP_{\text{derived}}$  and  $XP_{\text{derived}}$ .

**Data analysis.** To enable qualitative and quantitative comparisons, the waveforms of aortic BP,  $AR_{\text{direct}}$ ,  $RP_{\text{derived}}$ ,  $XP_{\text{derived}}$  and  $XP_{\text{direct}}$  were scaled to share the same relative amplitude and expressed in arbitrary units. To do this, each waveform (X) was scaled to its comparator waveform (Y) by first calculating the minimum (minY) and maximum (maxY) values of waveform (Y) as well as the minimum (minX) and maximum (maxX) values of each waveform (X). To derive the scaled waveforms, the formula  $(\text{minY} + (X - \text{minX}) * (\text{maxY} - \text{minY}) / (\text{maxX} - \text{minX}))$  was solved for each. All waveforms were then (in various permutations as described below) plotted across the full cardiac cycle before quantitative analysis of relationships was performed. Pearson product-moment correlation coefficients were calculated by comparing individual data points (~3000 per waveform). These calculations were made using statistics software (IBM SPSS statistics for windows, version 20.0, Chicago, IL) and  $P < 0.05$  was considered statistically significant. To quantify the linear correlation and temporal relationship between waveforms, cross-correlation analysis was employed using the method outlined in Nelson-Wong et al.<sup>6</sup> The cross-correlation coefficient at a phase lag of zero represents the overall concordance between the two waveforms analysed, and is comparable to the standard Pearson correlation coefficient (e.g. a cross-correlation of 1.0 represents perfect correlation and 0 represents no correlation). The peak cross-correlation coefficient represents the maximum temporal concordance between waveforms during iteration (or ‘phase shift’), allowing precise calculation of the delay (or ‘phase lag’) at which the peak cross-correlation (similarity) in waveforms occurred (e.g. a phase lag of 0 seconds represents perfect temporal association). Cross-correlation analysis was performed using custom and inbuilt functions of STATA for windows, version 12.1, StataCorp, College Station, TX.

## References

1. Schultz MG, Davies JE, Roberts-Thomson P, Black JA, Hughes AD, Sharman JE. Exercise central (aortic) blood pressure is predominantly driven by forward traveling waves, not wave reflection. *Hypertension*. 2013;62:175-182
2. Davies JE, Whinnett ZI, Francis DP, Willson K, Foale RA, Malik IS, Hughes AD, Parker KH, Mayet J. Use of simultaneous pressure and velocity measurements to estimate arterial wave speed at a single site in humans. *Am J Physiol Heart Circ Physiol*. 2006;290:H878-885

3. Davies JE, Hadjiloizou N, Leibovich D, Malaweera A, Alastruey-Armon J, Whinnett ZI, Manisty CH, Francis DP, Aguado-Sierra J, Foale RA, Malik IS, Parker KH, Mayet J, Hughes AD. Importance of the aortic reservoir in determining the shape of the arterial pressure waveform – the forgotten lessons of Frank *Artery Research*. 2007;1:40-45
4. Wang JJ, O'Brien AB, Shrive NG, Parker KH, Tyberg JV. Time-domain representation of ventricular-arterial coupling as a windkessel and wave system. *Am J Physiol Heart Circ Physiol*. 2003;284:H1358-1368
5. Abel FL. Maximal negative dp/dt as an indicator of end of systole. *Am J Physiol*. 1981;240:H676-679
6. Nelson-Wong E, Howarth S, Winter DA, Callaghan JP. Application of autocorrelation and cross-correlation analyses in human movement and rehabilitation research. *J Orthop Sports Phys Ther*. 2009;39:287-295